X-ray computed tomographic and focused ion beam/electron microscopic investigation of coating defects in niobium-coated copper superconducting radio-frequency cavities.

S. Aliasghari[a,b,c], P. Skeldon[b], X. Zhou[b], A. Gholinia[b], X. Zhang[d,e], R. Valizadeh[a], C. Pira[f], T. Junginger[g,h] , G. Burt[i,j], P. J. Withers[d].

[a]*ASTeC, STFC Daresbury Laboratory, Daresbury, Warrington, Cheshire WA4 4AD, UK.*

[b]*Department of Materials, The University of Manchester, Manchester M13 9PL, UK.*

[c]*Iranian Light Source Facility, ILSF, Institute for Research in Fundamental Sciences, IPM, Tehran, Iran*

[d]*Henry Moseley X-ray Imaging Facility, The Henry Royce Institute, Department of Materials, The University of Manchester, Manchester, M13 9PL, UK.*

[e]*Department of Engineering Science, University of Oxford, Parks Road, Oxford OX1 3PJ, UK.*

[f]*Legnaro National Laboratories INFN, Legnaro, Italy*

[g]*Department of Physics and Astronomy, University of Victoria, Victoria, BC V8P 5C2, Canada.*

[h]*TRIUMF, 4004 Wesbrook Mall, Vancouver, BC V6T 2A3, Canada.*

[i]*Engineering Building, Lancaster University, Lancaster, LA1 4YW, UK.*

[j]*Cockcroft Institute, Keckwick Ln, Daresbury, Warrington, WA4 4AD, UK.*

Abstract

A combination of X-ray computed tomography (CT) and focused ion beam - scanning electron microscopy (FIB-SEM) is employed to investigate substrate and related surface defects in a niobium coated superconducting radio frequency (SRF) copper cavity. The cavity was manufactured by spinning, with subsequent application of a sputtering-deposited niobium coating ($\approx$ 40 µm thick) on the internal surface. Before coating, the copper surface was pre-treated in several stages, ending with chemical polishing. CT and FIB-SEM identified furrows ($\approx$ 20 µm deep) in the copper beneath the coating, with an alignment consistent with remnants of score lines from the spinning process. The furrows were filled with niobium and contained voids at the niobium/copper interface that extended a few microns into the niobium coating. The presence of the defects led to similar furrows at the niobium surface. The study reveals the importance of pre-treatment of the cavity internal surface to avoid defects that may have deleterious influence on the Q slope and durability of the niobium coating.

Keywords: SRF Cavity, coating, CT, FIB-SEM, superconductivity, niobium

Introduction

The development of surface treatments of bulk (monolithic) niobium superconducting radio frequency (SRF) cavities for use in particle accelerators has increased the accelerating field from a few MV m^{-1} to over 40 MV m^{-1} [1]. Bulk niobium cavities are typically limited by the poor thermal conductivity of niobium and the requirement to have a finite wall thickness to limit mechanical deformation and vibration. The poor thermal resistance to liquid helium results in increased temperatures, which cause a rise in the electrical (BCS) resistance of the niobium surface leading to thermal runaway. There has been significant interest in the use of copper cavities with thin film (~micron) niobium coatings [2, 3] to benefit from the increased thermal conductivity of copper. Thin film coated cavities can sometimes show decreased surface resistance at low fields compared with bulk cavities, but usually have a sharp increase in surface resistance as the field increases (known as Q slope), which is not fully understood [4].

At 0.4 GHz and 4 K, the BCS surface resistance of clean niobium is around 42 nΩ compared with 40 nΩ at low field and 60 nΩ at high field for a bulk cavity, while for a thin film cavity the surface resistance is initially similar, but rises to hundreds of nΩ by a few tens of mT surface magnetic field [4]. Both effects were originally believed to be due to the lower residual resistance ratio (RRR) of the thin films (typically 10-30). The surface resistance is strongly dependant on the mean free path, with very clean (bulk) and very dirty samples having higher resistance than materials with intermediate mean free paths [5]. The thermal resistance is also limited by the RRR causing the temperature increasing steeply with increasing field. However, to date attempts to remove the Q slope due to higher RRR films have not been successful.

Recently it has been proposed that the Q slope is due to voids between the niobium/copper interface [6]. As the film is very thin the thermal conducting path around the void is longer than the path were there no void leading to insufficient cooling and an increase in temperature. One way around these effects is to use a thick film coating (around tens of microns). This has two effects, first the RRR is shown to increase with film thickness, and secondly the path around voids is not significantly lengthened. Initial results have shown that this approach can reduce the Q slope significantly [6]. The effect of defects at the sputtered niobium/copper interface on the Q factor has been addressed in a recent model that is based on high local

thermal resistances between the coating and the copper due to imperfect coating adhesion or other sources of defects that result in an imperfect thermal contact at the interface [7].

For monolithic cavities surface treatment of the cavity walls is critical in order to remove damage layers produced during fabrication (e. g. sheet rolling and cell stamping or hydro-forming or spinning). These layers can be 100–200 μm deep [8]. Saito [9] showed that to obtain a high field gradient of 30 MV m^{-1} the surface roughness should be reduced to < 2 μm. Similar considerations apply to thick film niobium-coated copper cavities, since the morphology and the roughness of the copper surface may affect the roughness of the niobium coating. However, for copper cavities, less information is available on the effects of surface preparation compared with monolithic niobium cavities and hence, the preparation process requires further by the SRF community.

In the present work, x-ray computed tomography (CT) is combined with focused ion beam – scanning electron microscopy (FIB-SEM) to identify defects in a niobium-coated copper cavity (see Fig 1a). This combination of approaches has not been applied previously to the examination of such defects. X-ray CT enables 3D-imaging and virtual cross-sectioning of the coating and substrate to identify the size, location and distribution of defects, which is not readily achievable by conventional 2D microscopy. Specific defects can then be selected and sectioned by FIB milling, for more detailed SEM examination of local composition and morphology.

Experimental

A 6 GHz niobium-coated copper cavity was selected randomly from ones produced in a INFN-CERN-STFC collaborative project [6, 7] The cavities were manufactured from 400 mm dia, 3 mm thick, planar copper blanks (99.9%) by spinning, as described in [10]. The inner surface of each cavity was (i) ground using coarse and fine abrasive particles, (ii) degreased in a surfactant solution and rinsed in deionized water, (iii) electropolished in 85% phosphoric acid/butanol, (iv) chemically polished in a sulfamic acid/hydrogen peroxide ammonium citrate/n-butanol solution, (v) passivated in a sulfamic acid solution and rinsed in high pressure ultrapure water. However, examination of several cavities indicated that the surface pre-treatment did not remove deeper scratches left by the spinning die (see Figs. 1(b, c). An approximately 40 μm thick niobium (RRR300) was then deposited by magnetron sputtering

[6]. The coating conditions are listed in Table 1 [6]. A multilayer deposition process was selected to mitigate the film stress. Full details are of the surface treatment and coating deposition process are provided in [6].

Table 1: Deposition conditions for the niobium coating.

Substrate heating	650°C for 12 h
Base pressure at 650°C	$<10^{-9}$ mbar
Deposition temperature/time	650°/8 h
Discharge gas/pressure	Ar/1.5×10^{-3} mbar
No of layers	140
Deposition rate at cell centre	1.45 nm s^{-1}

Examination of the niobium-coated copper by SEM utilized a Zeiss Ultra 55 instrument, equipped with energy dispersive X-ray (EDX) analysis facilities and a FEI Magellan HR FEG-SEM equipped with a Forward Scatter Detector (FDS).

X-ray CT was undertaken using a Zeiss Xradia Versa 520 lab-based X-ray CT scanner, at an accelerating energy of 140 keV, which generated a polychromatic X-ray beam. An LE5 (doped glass) filter was used to improve the X-ray transmission rate. A sample of area 4 x 2 mm was excised from the cavity (see Fig 1 a) for CT scanning. A total number of 2001 projections were taken over 360° rotation. The 4× optical lens behind the scintillator combined with geometric magnification resulted in an effective voxel size of (1.89 μm). The data were reconstructed using Zeiss Xradia Reconstruction software, which is based on a filtered back-projection algorithm. Once the data were reconstructed, a nonlocal LE5 means filter was applied to the data set to reduce noise. This was followed by a semi-automated segmentation procedure, using Avizo software, which could reliably identify defects based on the greyscale level and the size of the defects. The niobium/copper interface was identified in terms of the gradient of the greyscale CT image and the regions segmented based on a grey value threshold.

Cross-sections of the coating at specific defective regions were prepared using an FEI Quanta 3D dual beam Ga$^+$ FIB-SEM. The selected area was coated with platinum to prevent irradiation damage during milling.
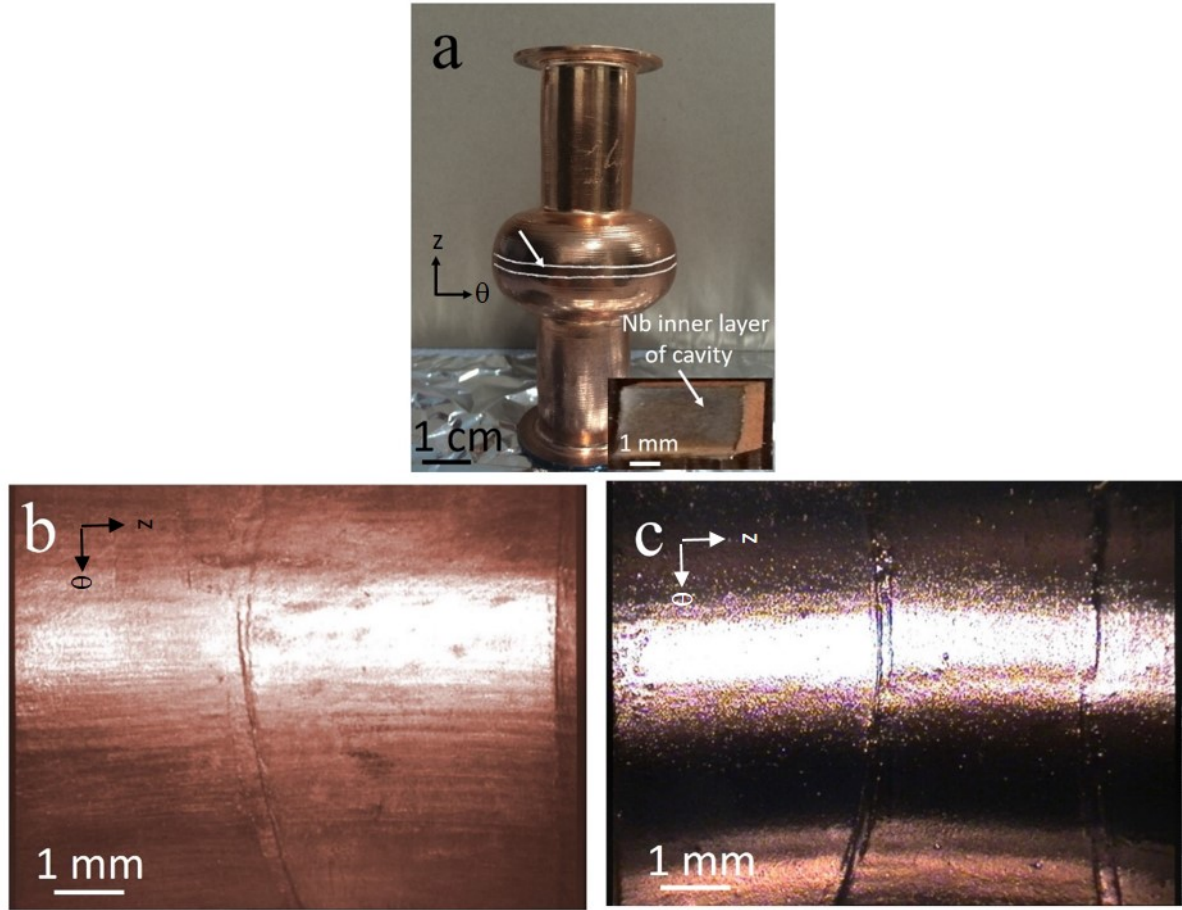
Results and discussion

Fig. 1 (a) Photograph of a 6 GHz resonant cavity. The arrow indicates the location of the sample used for X-ray CT and FIB. The sample is shown enlarged in the inset. (b) Optical image of the inner surface of an as-spun cavity and (c) an image of an inner surface after grinding, electropolishing and chemical polishing. The circumferential (θ) and axial (z) directions of the cavity are indicated.

Fig. 2 (a, b) shows low and high magnification SEM micrographs of the surface of the niobium coating on the inner surface of the cavity. The surface mainly consists of elongated crystal facets, typically about 1 - 5 μm long and 1 - 2 μm wide, with an apparently random orientation.

The surface uniformity was occasionally disrupted by furrow-like defects (Fig. 2 (b)). These had lengths of several tens of microns and widths ≈ 5 to 10 μm.
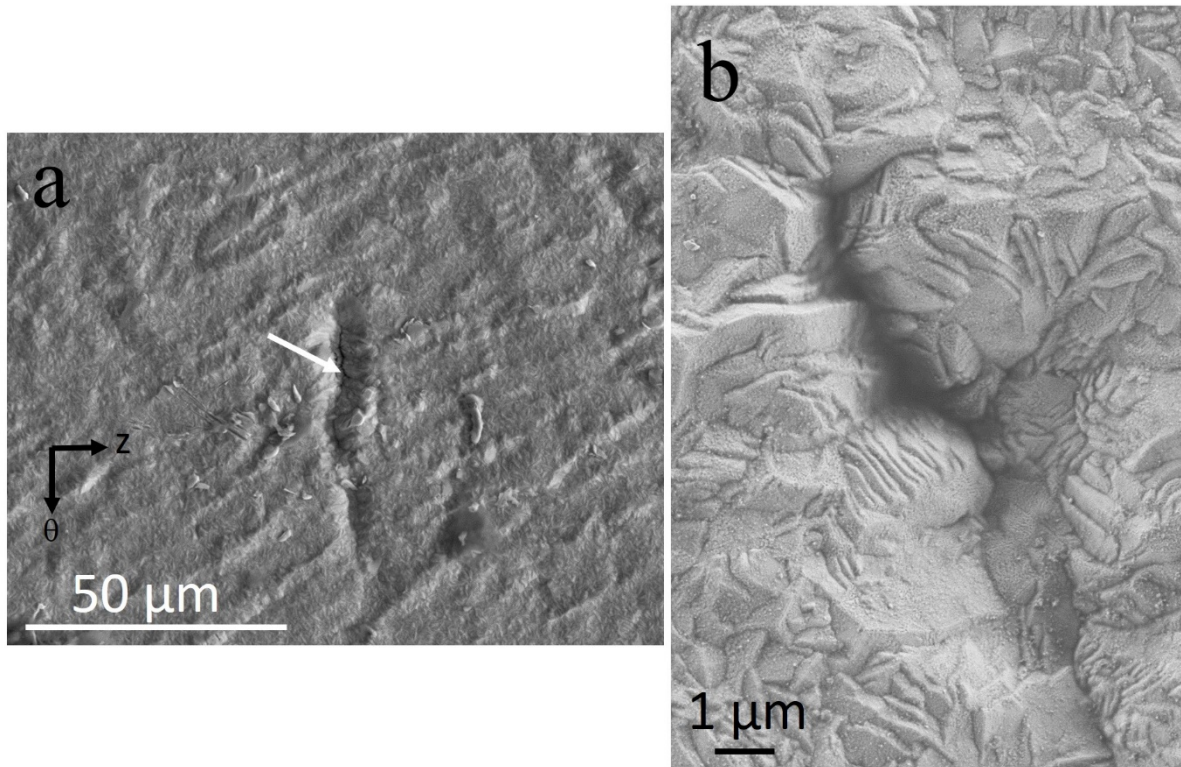

Fig. 2. (a) SEM of a furrow-like defect visible on the niobium surface of the sample from the cavity. (b) Defect at higher magnification.

In order to identify whether the occurrence of the furrow-like surface defects on the surface of the niobium coating are correlated to ones on the surface of the copper substrate, X-ray CT mapping of the niobium surface and the niobium/copper interface was carried out. In each case the boundary was identified and a height map of the boundary relative to a plane approximately parallel to the coating constructed as shown in Figure 3a. In each case deviations from that plane are represented as colours with 0 μm represented blue. Undulations are evident as red hotspots. The maps in Fig. 3a show the deviations in the height of the coating surface (left) and the Ni/Cu interface (right) over an ≈ 1 x 2 mm area of the sample removed from the central region of the cavity. Owing to the concavity of the sample, the green region at the centre of the sample reflects the sample curvature which lie around 7 to 15 μm and 10 to 15 μm and below the sample edges, for the niobium surface (left) and the niobium/copper interface (right) respectively. The depth changes across the area of the two boundaries are similar as would be

expected for a coating that replicates closely the surface topography of the substrate. The lateral banding in the maps is probably due to the surface height variations in the copper substrate created by the spinning fabrication process that remains following application of the niobium coating. The black rings mark the locations of hotspots that are roughly 5 to 10 μm deeper than the immediate surrounding regions. It is clear that the depressions in the top surface correlate strongly with depressions at the Cu-Ni interface. Further, these sites tend to be elongated along the circumferential direction and are parallel to the lateral banding, suggesting their origin in the process by which the cavity is manufactured. They have lengths between 20 to 100 μm and are separated by distances of several hundred microns.

It is evident from the virtual X-ray CT cross-section in Fig. 3 (b) that the average thickness of the niobium layer is 42 μm. The surface depression in the niobium is about 30 μm wide and 7 μm deep, and coincides with a bright feature, of similar dimensions, which penetrates into the copper at the niobium/copper interface. This is shown by subsequent FIB sectioning, presented below, to be a furrow in the copper substrate that contains niobium and also voids. The brightness of the feature is possibly an effect of increased X-ray scattering from the void and furrow interfaces. Fig. 3 (d) shows an extended length of the virtual cross-section. Three defects similar to the one shown in Fig. 3 (c) are revealed that are separated by a distances of 1090 and 640 μm which corresponds to the spacing of the defects in the X-ray CT map.
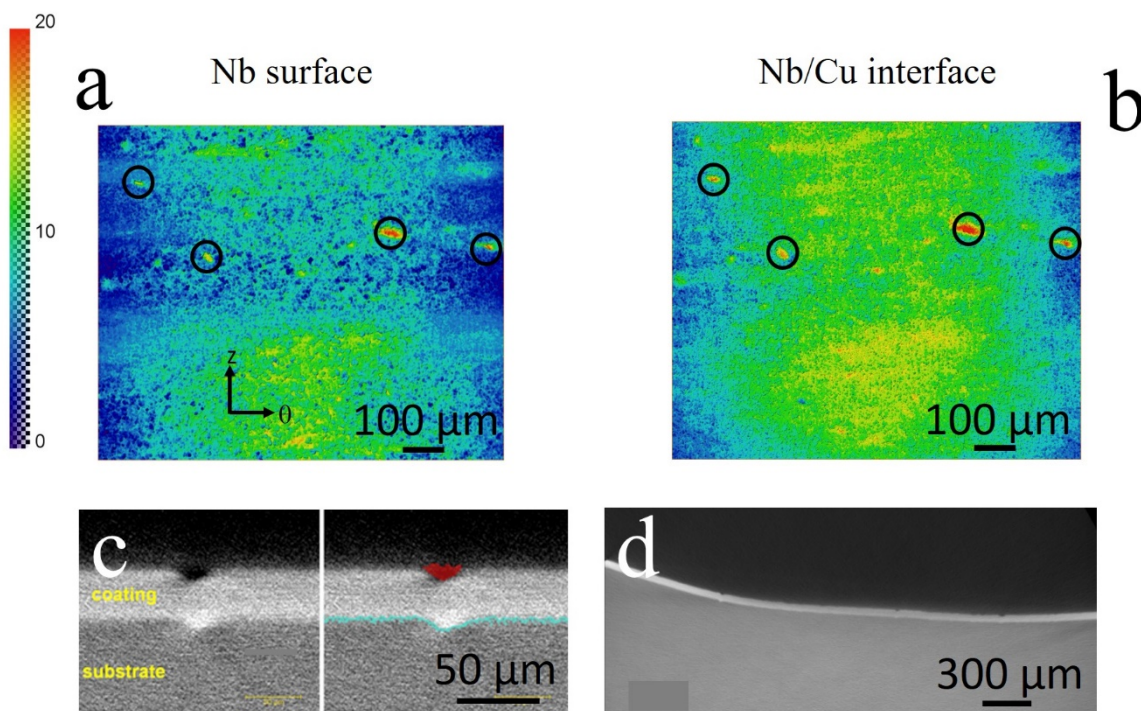
Fig. 3. (a) Height map over a region of interest for the top surface of the niobium (left) and the corresponding height map for the underlying niobium/copper interface (right) deduced from the X-ray tomogram. Rings highlight depressions in the copper that coincide with those in the niobium surface. (b) Virtual CT cross-section showing a depression in the niobium coincident with a corresponding depression in the copper substrate. (c) Virtual cross-section showing three similar examples, separated by several hundred microns. The vertical and horizontal arrows in (a) indicate the axial and circumferential directions, respectively.

The cross-sections shown in Fig. 4 exemplify the observation that the defect in the Cu-Nb interface translates through to essentially the same scale of defect the coating surface. In this instance, the defect is about 22 μm wide at its widest point and about 90 μm in length. Furthermore, the defect is elongated in the circumferential direction.
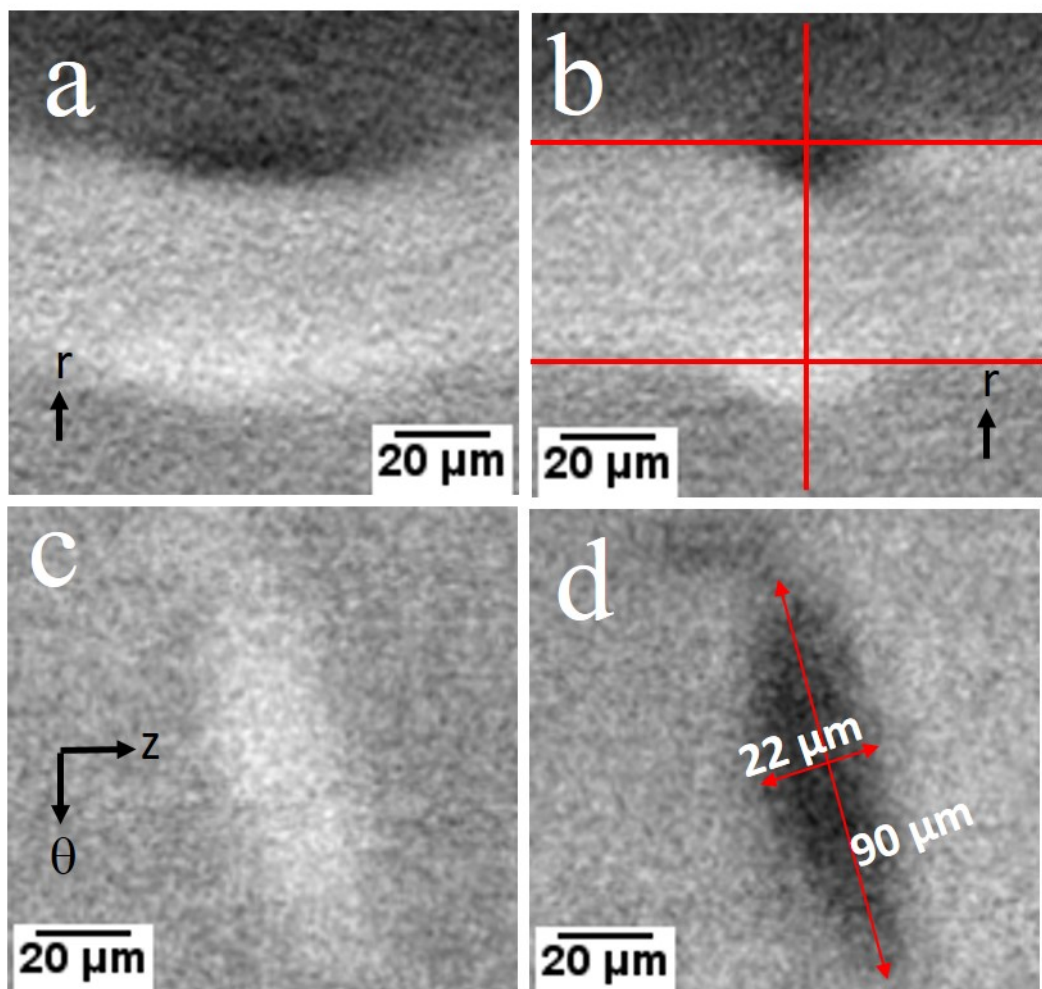

Fig. 4. Virtual CT slices of a single defect. (a, b) Axial and circumferential cross-sections of the niobium-coated copper, respectively. (c) Top of the niobium coating. (d) Bottom of the niobium coating.

FIB milling was used to study the defect observed in Fig 1 in more detail. Prior to milling the top surface was protected by a (5 – 10 μm wide) Pt capping strip deposited transversely across the surface furrow prior to sectioning (Fig 5a). It is clear from Fig 5c that the voids are located within the corresponding furrow at the niobium/copper interface. The furrow is ≈ 25 μm wide and ≈ 3.5 μm deep . It lies directly beneath the furrow at the coating surface, which is ≈ 10 μm wide and 4 μm deep. The coating thickness is ≈ 42 μm is in agreement with the result from X-ray CT.
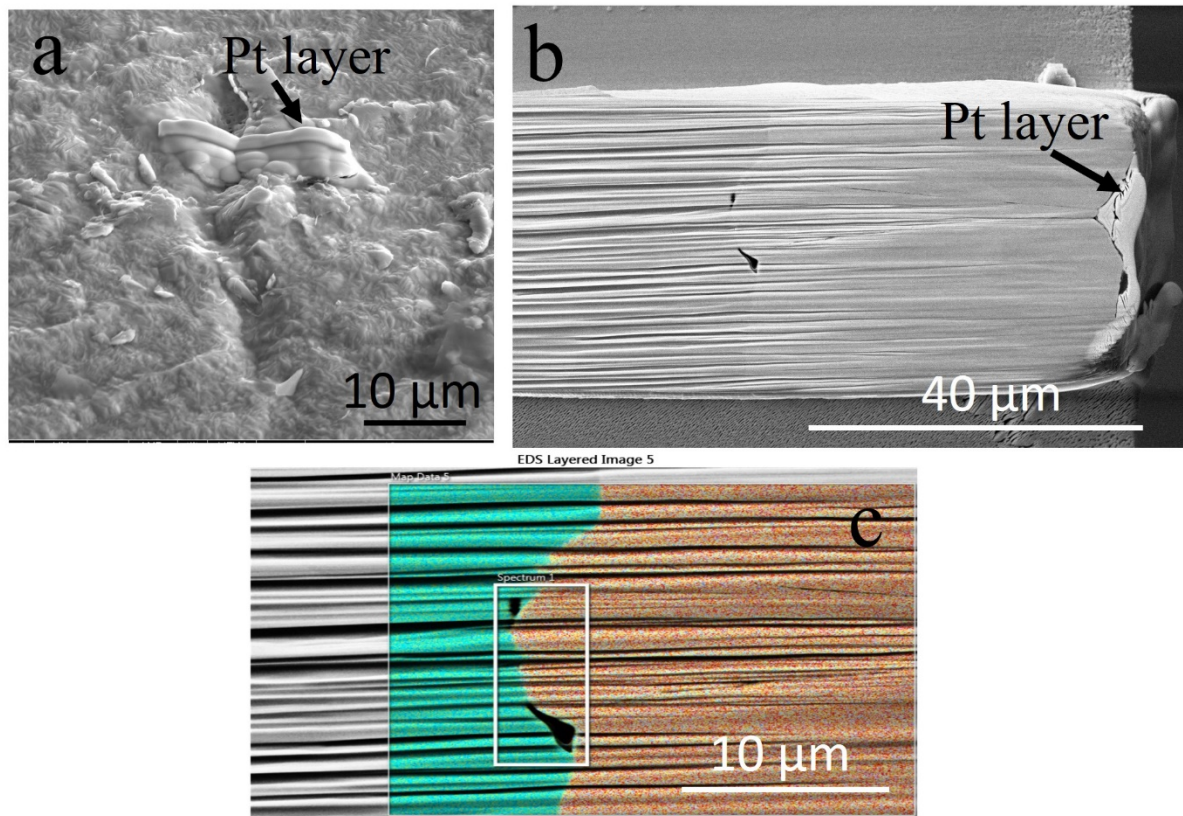

Fig. 5 (a) Scanning electron micrograph of the surface of the niobium coating showing the position of the platinum strip applied to protect the surface furrow prior to FIB milling. (b) micrograph of the ion beam milled, laser trimmed and further ion beam milled cross-section of the niobium-coated copper. (c) Superimposed EDX map (niobium (brown) and copper (turquoise)) showing the location of the voids in the vicinity niobium/copper interface.

Fig. 6 confirms the observation from Fig. 5 that the voids (appearing as dark features) are located near the niobium/copper interface (see arrows). The defect extends into the niobium above the voids as a region of darker appearance relative to the niobium coating due to reduced secondary electron emission (Fig. 6 (b)). The EDX maps suggest that the voids at the

niobium/copper interface are partly covered by a thin layer of copper, which may have been displaced during spinning and not fully removed by the surface treatment. Linear features, possibly consisting of fine voids, are also revealed above the void region within the overlying niobium layer,. Similar features, apparently remote from an interfacial defect, are evident in the niobium in Fig. 6 (a). The voids at the niobium/copper interface appear to be partly filled by a thin niobium layer, with a thickness in the range ≈ 50 to 400 nm. The thickness range is of the order of the thickness of one of the sequentially-deposited niobium layers, ≈ 300 nm. Such filling may arise when cavities formed by displaced copper are open to ingress of sputtered niobium. However, it is not possible to eliminate that the layers originate from re-deposition of niobium during sputtering. Fig. 6 (e) shows the same defect region as Fig. 6 (a) following further ion beam milling. The additional milling has exposed more void regions (see arrows) both at the niobium/copper interface and also in the defect region above the interfacial voids, where the milling has removed a thin layer of material that covered the defect in Fig. 6 (b). The defect extends into the niobium by ≈ 3 μm distance from the substrate.
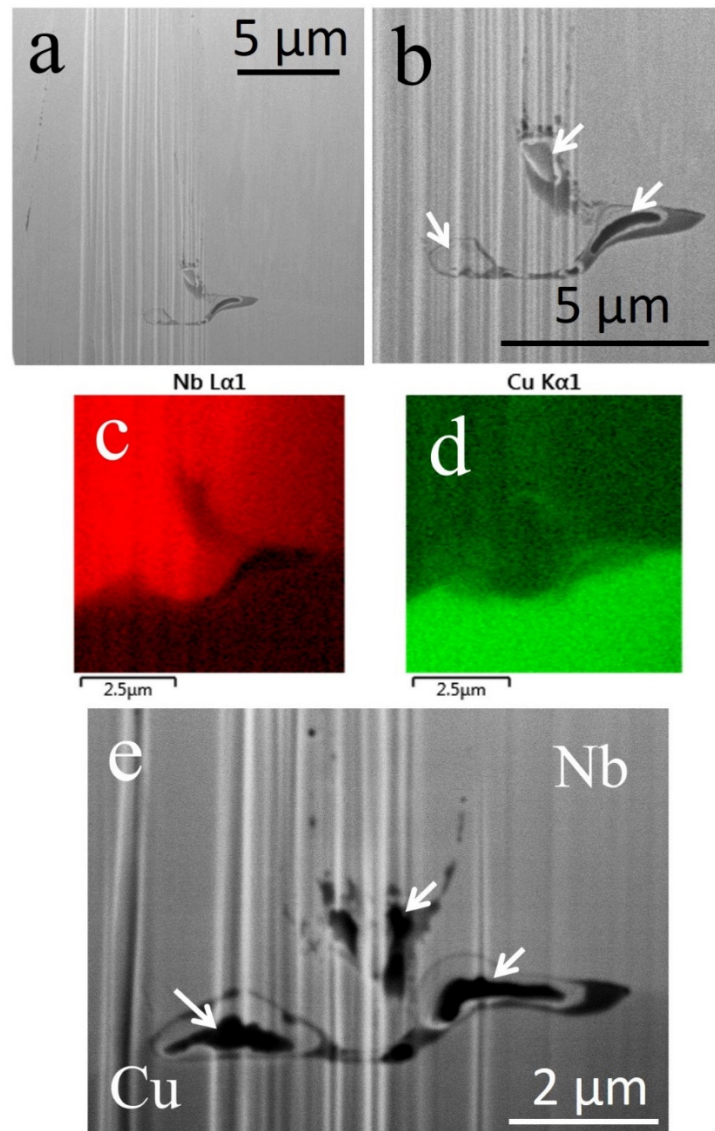
Fig. 6. (a) Secondary electron micrograph of the ion-beam milled cross-section of the niobium-coated copper, prior to laser trimming. Final milling was carried at using a nA ion beam to minimize beam damage and contamination. (b) Details of the defect near the niobium/copper interface. (c, d) EDX maps of niobium and copper, respectively. (e) Defect region after additional ion milling.

The present results suggest that spun copper surface contains regions furrows created by the shaping tool. The cavities maybe formed preferentially at the furrows by copper being displaced across the furrow edges by the spinning die. Thin layers of displaced copper may also project from the substrate, forming sites for the extension of defects into the niobium layer. The latter may then give rise to cavity formation by shielding during sputtering of the niobium.

The work shows the importance of surface finishing for the minimization of defects in the superconducting layer.

Conclusions

The results of the study show that even with the extensive surface preparation procedure applied to the copper, large defects may remain in the internal wall of the SRF cavity. These defects can be readily identified and characterized by X-ray CT and FIB-SEM, which shows a correlation between surface defects in the niobium coating and the underlying defects in the substrate. The defects in the copper probably originate from the spinning process that leaves scratches that are too deep for complete removal by the applied surface pre-treatments. The defects at the niobium/copper interface are likely to be sites of impaired heat transfer and could possibly affect the durability of the coating during cavity operations.

Acknowledgements

References

[1] H. Padamsee, SRF accelerators flourish in a golden age, 6th International Particle Accelerator Conference, Richmond, VA, USA, May 3-8 (2015).

[2] A. Sublet, W. Venturini Delsolaro, M. Therasse, T. Richard, G. Rosaz, S. Aull, P. Zhang, B. Bártová, S. Calatroni, M. Taborelli, Developments on SRF Coatings at CERN, (2015): Proc. 17th Int. Conf. on RF Superconductivity (SRF2015), Whistler, BC, Canada, Sept. 13-18, 2015, paper TUPB027, pp. 1-5.

[3] A.I. Sublet, A. Aviles, N. Jecklin, P. Costa Pinto, S. Calatroni, A. Sapountzis, W. Venturini Delsolaro, W. Vollenberg, and S. Prunet, Thin film coating optimization for HIE-ISOLDE SRF cavities: coating parameters study and film characterization, Proc. 16th Int. Conf. on RF Superconductivity (SRF2013): Paris, France, Sept. 23-27, 2013, paper TUP077, pp. 623-626,.

[4] S. Aull, W. Venturini Delsolaro, T. Junginger, Anne-Marie Valente-Feliciano, Jens Knobloch, Alban Sublet, and Pei Zhang, On the understanding of Q-Slope of niobium thin films, Proc. 17th Int. Conf. on RF Superconductivity (SRF2015), Whistler, BC, Canada, Sept. 13-18, 2015 paper TUBA03, pp. 494-500.

[5] J.T. Maniscalco, D. Gonnella, and M. Liepe, The importance of the electron mean free path for superconducting radio-frequency cavities. J. Appl. Phys. 121 (2017): 043910.

[6] C. Pira, Nb thick films in 6 GHz superconducting resonant cavities, PhD thesis, (2018).

[7] V. Palmieri, R. Vaglio, Thermal contact resistance at the Nb/Cu interface as a limiting factor for sputtered thin film RF superconducting cavities, Supercond. Sci. Technol. 29 (2016) 015004 (12pp).

[8] P. Kneisel, K. Saito, and R. Parodi, Performance of 1300 MHz KEK-type single cell niobium cavities, Proc. 8th Int. Workshop on RF Superconductivity (SRF1997), Abano Terme (Padova), Italy, Oct. 6-10, 1997, paper SRF97C07, pp. 463-471.

[9] K. Saito, Surface smoothness for high gradient niobium SC RF cavities", Proc. 11th Workshop RF Superconductivity (SRF'03), Lübeck, Germany, Sept. 8-12, 2003, paper THP15, pp. 637-640.

[10] V. Palmieri, Advancements on spinning of seamless multicell reentrant cavities, Proc. 11th Int. Conf. on RF Superconductivity (SRF2003), Lübeck/Travemünder, Germany, Sept. 8-12, 2003, paper TUP26, pp. 357–361.

Fig. captions

Fig. 1 (a) Photograph of a 6 GHz resonant cavity. The arrow indicates the location of the sample used for XCT and FIB. The sample is shown enlarged in the inset. The horizontal and vertical arrows in (a) indicate the directions designated circumferential and axial, respectively. (b) Optical image of the inner surface of an as-spun cavity and (c) and of an inner surface after grinding, electropolishing and chemical polishing.

Fig. 2. (a) Scanning electron micrograph of a defect in the niobium surface of the sample of Fig. 1. (b) Defect at higher magnification.

Fig. 3. (a) XCT height map in a plane approximately coincident with the niobium surface. Depressions in the surface are shown in red. (b) XCT height map at the niobium/copper interface. Rings highlight depressions in the copper that coincide with those in the niobium surface. (c) Virtual cross-section showing a depression in the niobium coincident with a depression in the copper substrate. (d) Virtual cross-section showing three similar examples, separated by several hundred microns. The vertical and horizontal arrows in (a) indicate the axial and circumferential directions, respectively.

Fig. 4. XCT virtual planar slices of a defect. (a, b) Axial and circumferential cross-sections of the niobium-coated copper, respectively. (c, d) Top of the niobium coating. (d) Base of the niobium coating.

Fig. 5 (a) Scanning electron micrograph of the surface of the niobium coating showing the position of the platinum strip applied at a surface furrow prior to FIB milling. (b) Micrograph of the ion beam milled, laser trimmed and further ion beam milled cross-section of the niobium-coated copper. (c) Superimposed EDX maps of niobium (brown) and copper (turquoise) showing the location of voids in the vicinity niobium/copper interface.

Fig. 6. (a) Scanning electron micrograph of the ion-beam milled cross-section of the niobium-coated copper, prior to laser trimming. Final milling was carried at using a nA ion beam to minimize beam damage and contamination. (b) Details of the defect near the niobium/copper interface. (c, d) EDX maps of niobium and copper, respectively. (e) Defect region after additional ion milling.